arXiv:2207.14696v2 [cs.LG] 17 Feb 2023

# BiFeat: Supercharge GNN Training via Graph Feature Quantization

**Yuxin Ma**
University of Science and Technology of China
leeadama@mail.ustc.edu.cn

**Ping Gong**
University of Science and Technology of China
gpzlx1@mail.ustc.edu.cn

**Jun Yi**
University of Nevada
junyi@nevada.unr.edu

**Zhewei Yao**
Microsoft
zheweiyao@microsoft.com

**Cheng Li**
University of Science and Technology of China
chengli7@ustc.edu.cn

**Yuxiong He**
Microsoft
yuxhe@microsoft.com

**Feng Yan**
University of Houston
fyan5@central.uh.edu

## Abstract

Graph Neural Networks (GNNs) is a promising approach for applications with non-Euclidean data. However, training GNNs on large scale graphs with hundreds of millions nodes is both resource and time consuming. Different from DNNs, GNNs usually have larger memory footprints, and thus the GPU memory capacity and PCIe bandwidth are the main resource bottlenecks in GNN training. To address this problem, we present BiFeat: a graph feature quantization methodology to accelerate GNN training by significantly reducing the memory footprint and PCIe bandwidth requirement so that GNNs can take full advantage of GPU computing capabilities. Our key insight is that unlike DNN, GNN is less prone to the information loss of input features caused by quantization. We identify the main accuracy impact factors in graph feature quantization and theoretically prove that BiFeat training converges to a network where the loss is within $\epsilon$ of the optimal loss of uncompressed network. We perform extensive evaluation of BiFeat using several popular GNN models and datasets, including GraphSAGE on MAG240M, the largest public graph dataset. The results demonstrate that BiFeat achieves a compression ratio of more than 30 and improves GNN training speed by 200%-320% with marginal accuracy loss. In particular, BiFeat achieves a record by training GraphSAGE on MAG240M within one hour using only four GPUs.

## 1 Introduction

Graph Neural Networks (GNNs) is a promising approach for modeling the structural information of data. Popular GNN models such as GraphSAGE[23], GCN[29], and GAT[42] have recently achieved state-of-the-art (SOTA) performance in a broad range of fields, such as social network[45], knowledge graph[47], recommender system[27], and bioinformatics[10].

Preprint. Under review.

However, training GNNs on large graphs (e.g., graphs with hundreds of millions of nodes) is non-trivial because of the expensive computation and memory demands during the training process. Deep network structure [32, 9] benefits GNN performance, but is also more demanding in computing and memory resources, especially when deployed in GPUs where the memory capacity is usually limited.

GNN training has a unique data pipeline. First, GNNs inherits the irregular data processing flow of graph analytics as the input nodes feed to the network are randomly sampled. Second, the computing pattern is regular and fast as the forward, backward, parameter update operations are the same across iterations and the computing is fast due to the relatively small number of parameters of GNNs compared to Deep Neural Network (DNNs). The dynamic and irregular data accesses combined with the regular and fast computation lead to frequent data loading, which causes poor CPU/GPU utilization as the computation is often waiting for data feeding.

To tackle these challenges, we propose BiFeat, a graph feature quantization method that accelerates GNN training by reducing the memory footprint and PCIe bandwidth requirement of graph features without compromising the training accuracy. Our key observation here is that GNNs features have much higher tolerance to quantization error compared to DNNs, thanks to the averaging during neighbor information aggregation, where errors can cancel out. To better understand the performance impact of graph feature quantization, we theoretically prove the convergence of BiFeat with a statistical bound on loss compared to the uncompressed network training and give the key factor.

In summary, we make the following main contributions:

- We make an initial effort on accelerating GNN training by performing feature quantization, and identify the main performance impact factors in graph feature quantization.
- We propose a graph feature quantization method BiFeat and make theoretical analysis on its convergence. BiFeat in general and can be used with any GNN models.
- Extensive experimental evaluation using various GNN models and datasets demonstrate that BiFeat achieves a compression ratio of more than 30, which improves GNN training speed by 50-200% with less than 1% accuracy loss. In particular, BiFeat achieves a record by training GraphSAGE on MAG240M within one hour using only four GPUs.

## 2 Background and Motivation

### 2.1 GNN Mini-batch Training

Graph Neural Networks (GNNs) extracts graph structure information by aggregating other nodes' features. Production-scale graphs are usually very large with a giant number of nodes and edges, as well as the associated features. For instance, as shown in Table 1, the MAG240M graph dataset consists of more than 240 million nodes and 3.4 billion edges, where each node has 768 features. Its total size is more than 349 201.7 GB, largely exceeding the GPU memory space (up to 80 GB) of the most advanced, commercially available GPU [36]. Therefore, it is impossible to fit the graph structure and features into the GPU memory for doing full graph training.

To address the limited GPU memory challenge, GraphSAGE[23], GCN-based FastGCN[8], and ClusterGCN[11] do not use full graph training, instead, introduce mini-batch training for GNNs. The core idea of GNN mini-batch training is to use a sampler to extract a subgraph from the full graph at each step and load the subgraph on GPU for training. We have been witnessing that it has been widely adopted, and become the native training method supported by the mainstream GNN training frameworks such as DGL[43] and PyG[18]. Though being able to train GNNs over large graphs, the mini-batch training suffers a serious data loading problem. This is because, during the training process, the structure information of the sampled subgraph and the corresponding features need to be continuously moved from CPU memory to GPU memory via PCIe, which is very slow due to the mismatch between the limited PCIe bandwidth and the large volume of transferred data. This would lead to waste of the expensive GPU resources. We demystify the data loading problem below.

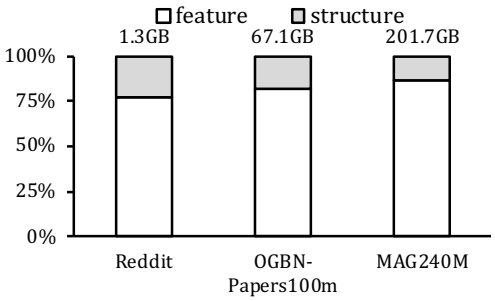



Figure 1: The ratios of feature and structure sizes of different datasets

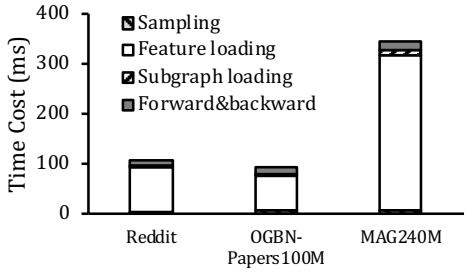



Figure 2: Breakdown of each phase of the mini-batch training of GraphSAGE on three datasets

### 2.2 Motivation

To conduct an in-depth analysis of the data loading pipeline, we train GraphSAGE [23] on Reddit, OGBN-Papers100M, and MAG240M datasets, with the training framework DGL. The statistics of these datasets can be found in Table 1. We summarize our key findings of below.

- Compared to the structure information, as shown in Figure 1, the feature data dominates the size of a graph dataset. For instance, for the largest graph MAG240M, its feature occupies 174 GB, accounting for 86.3% of its total size.
- The feature data loading is the bottleneck. Specifically, as illustrated in Figure 2, across the three training tasks, the feature loading time is 81%, 74%, and 91% of their training time costs, respectively. Furthermore, GNN models usually have a relatively small number of parameters compared to DNNs, thus the computation time of forward and backward propagation is very small compared to feature data loading. This also makes the feature data loading a very frequent task and difficult to be hidden by computation.
- In each iteration, input nodes are randomly sampled from a large set of nodes. Such randomness makes it challenging to utilize the spatial-temporal locality in data access. Thus the help from caching is usually limited.

The above patterns indicate that the GNN feature data loading is a random yet heavy workload. Due to the large scale of GNN feature data (hundreds of GB to TB), it is infeasible to store all raw GNN feature data in GPU memory. Storing features in CPU memory can address the limited GPU capacity issue but also causes a data movement bottleneck due to the frequent and heavy data loading. Thus, reducing the feature data size can greatly help relieve GPU memory and PCIe bandwidth pressure.

To reduce the feature data size, compression is a natural solution. The common compression techniques include sparsification [30, 3] and quantization [37, 44, 35]. For spasification, most graphs, especially large ones, have features in the form of float numbers, which is dense. Unlike this, quantization is more general, and can handle dense features. Therefore, our goal is to devise a new GNN feature quantization methodology to compress feature data so that the data volumes transferred between CPU memory and GPU memory have been greatly reduced. For quantization, our key insight is that GNNs features have much higher tolerance in reduced precision compared to DNNs as errors can be cancelled out by averaging during neighbor information aggregation. In this paper, we will provide both theoretical and practical results to support this observation.

### 2.3 Related Work

Here, we briefly iterate a few most relevant works that share the same goal of addressing the slow data pipeline challenge in GNNs as we do. PaGraph[31] utilizes spare GPU memory to cache frequently visited graph data to speed up data loading. However, due to the large GNN feature size, the sampling randomness, and the limited GPU memory, spare GPU memory can only cache a small portion of features, especially for large datasets. Therefore, such method does not scale well for large graphs, and observes diminished cache hit ratios and speedups with the increase in the graph size.

GNNAutoScale[17] supports large scale GNN training by using historical embedding instead of re-calculating neighbor's embedding at every step. This reduces GPU memory consumption and data loading time since less number of nodes are involved at each step. However, historical embedding increases CPU memory cost by a factor of the number of layers, results in poor scalability for large-scale datasets. Global sampling[15] aims at solving the data loading problem by using a small cache in GPU with higher sampling priority for nodes in cache. However, such method may lead to accuracy degradation and is also coupled with specific models. The modified forwarding method is also slower than the original one and thus limits the actual speedup. Existing works, such as Binary Graph Neural Networks[5], VQ-GNN[14], Sgquant[16], Degree-quant[39], also use quantization for GNNs. However, they focus on reducing the size of weights and activations, which is orthogonal to our work as we aim at addressing the data loading bottleneck by compressing the GNN features.

# 3 GNN Feature Quantization

Quantization has been widely used to reduce model size [14, 28, 33] and gradients [44], but applying it to GNN features has not been explored before. Given compressing feature data is different than compressing model or gradients, it is non-trivial to find an appropriate quantization method and understand the corresponding accuracy impact, compression benefits, and computation cost.

In this paper, we propose BiFeat: a GNN feature quantization methodology that supports both Scalar and Vector quantization approaches to accelerate GNN training by significantly reducing the memory footprint of GNN feature data. We first explore the Scalar quantization method (in Section 3.1), which is simple and compute-efficient. But its flip-side is the limited compression ratio of up to 32. To enable GNN training with extremely large graphs, in Section 3.2, we additionally investigate the validity of the vector quantization method [21], which can raise the compression ratio up to a few hundreds or thousands. However, this comes at the price of compute-intensive feature preprocessing. We give the implementation details of the two methods in Section 3. Following that, we give a theoretical analysis to prove their negligible impacts on training convergence and accuracy in Section 4. Finally, we run intensive experiments with state-of-the-art GNN models and various graph datasets to validate the effectiveness and efficiency of applying BiFeat to boost GNN mini-batch training over large graphs.

## 3.1 BiFeat-SQ

BiFeat Scalar quantization (BiFeat-SQ) projects continuous value to several discrete values, thus we can use a low bit width integer to indicate a float number [22]. BiFeat-SQ may cause a rounding error proportional to the gap between two discrete values. The commonly used uniform quantization method uniformly selects these values so that the gaps are even and the maximum rounding error is reduced. However, using it on graph features requires a different setup. Most large-scale graphs have features near normal distribution because features are usually outputs generated from models such as BERT[13]. Since most of the values are near zero, to reduce the overall rounding error, we use logarithm based quantization method:

$$Q(x) = \begin{cases} 2^{k-1} - 1 - \lfloor \frac{Clip(log_2(-x)) - e_{min}}{e_{max} - e_{min}} * 2^{k-1} \rfloor, & x < 0 \\ 2^{k-1} + \lfloor \frac{Clip(log_2 x) - e_{min}}{e_{max} - e_{min}} * 2^{k-1} \rfloor, & x \geq 0 \end{cases} \tag{1}$$

where *x* is the original feature, $e_{min}$ and $e_{max}$ are the minimum and maximum values respectively of binary logarithm on non-negative $x$ after clipping outlier values, i.e., $Clip(log_2|x|)$. This is actually a uniform quantization of the clipped logaritm. We tradeoff some dynamic range to reduce the overall rounding error. Dequantization is similar in a reversed manner:

$$Q^{-1}(q) = \begin{cases} exp2\left(\frac{(2^{k-1} - 0.5 - q) * (e_{max} - e_{min})}{2^{k-1}} + e_{min}\right), q < 2^{k-1} \\ exp2\left(\frac{(q - 2^{k-1} + 0.5) * (e_{max} - e_{min})}{2^{k-1}} + e_{min}\right), q \geq 2^{k-1} \end{cases} \tag{2}$$

where $q$ is the quantized value from equation 1.

Scalar quantization can compress and decompress quickly, but it has a maximum compression ratio of 32 when $k = 1$ and the sign of x is used for the quantized value (positive or non-positive). Such quantization method only slightly degrade the accuracy. We don't differentiate zero and negative

values for the compatibility of discrete original value like in one-hot code[34] and binary features[25]. For example, on tiny graph datasets like Cora[6] and Citeseer[29], quantizing these datasets would not bring much information loss.

### 3.2 BiFeat-VQ

BiFeat Vector quantization (BiFeat-VQ) views all GNN feature data as vectors and uses clustering methods such as kmeans to group features into clusters. It uses the clustering centers to present the values in the cluster [20]. These centers are stored in a codebook and the index can be used to indicate each value. BiFeat-VQ method can achieve a much higher compression ratio because it represents multiple float values with an integer. BiFeat-VQ is usually slower than BiFeat-SQ in quantization, though the dequantization speed is similar.

However, due to the GPU memory limitation, it is very difficult to directly quantize vectors with hundreds of dimensions through a large codebook with thousands of entries. Features need to be split into multiple parts with less dimensions, each part has a independent codebook. So the number of codebook entries and the length of each entry are two parameters in BiFeat-VQ, namely length and width. Besides these two parameters, another setting is using Euclidean distance or cosine similarity to measure the distance between vectors. These settings are critical for achieving a high compression ratio with little accuracy impact. Our experiments show that cosine similarity consistently performs better. This is because the relative size of different dimensions is more important. And less partition combined with large codebooks helps too.

BiFeat-VQ requires careful hyperparameters tuning, but can possibly reach a higher compression ratio. If the original feature bitwidth be $b$, we can calculate the theoretical compression ratio by $CR = width * b/log_2 length$. Due to bit alignment, The value of length may need to be carefully selected. Codebooks are usually far smaller than the quantized features, and we see increasing the length won't cause the compression ratio to drop too much.

### 3.3 System Integration

BiFeat performs feature quantization against the target graph datasets before training. This is one-time job, and can be re-used across multiple runs. At every training iteration, BiFeat loads quantized features, corresponding to a sampled subgraph, from CPU memory to GPU memory, and recovers compressed features into their correct formats by conducting dequantization on GPU, before kicking off the forward and backward computation. The dequantization is required as we want to make BiFeat be transparently integrated with the GNN training framework DGL, and keep the computation kernels unchanged with their input features with common formats. BiFeat significantly reduces the data loading size and thus accelerates the training. Since the data and its format loaded into the GNN model is unchanged, no modification is required in GNN models. Therefore, BiFeat can be easily implemented with only a few lines of code.

BiFeat also supports batching, which is especially useful when processing large scale graph like MAG240M. Specifically, BiFeat loads and dequantizes a small batch at a time to reduce the GPU memory consumption. Next, we detail BiFeat Scalar and BiFeat Vector quantization approaches.

## 4 Theoretical Analysis

We prove a graph neural network with sufficient width, starting from a random initialization and using input features with small quantization error, would eventually converge to a network where the loss suffered with input error is within $\epsilon$ of the optimal loss using original features.

We denote the input features as $X = (x_1, x_2, ..., x_N) \in \mathbb{R}^{N \times d}$, here $N$ is the number of nodes and $d$ is the number of feature dimensions. The features after quantization is $X' = (x'_1, x'_2, ..., x'_N) \in \mathbb{R}^{N \times d}$ satisfying $\|x_i - x'_i\|_2 \leq \delta, \forall i \in [N]$.

**Assumption 1 (Independent rounding error)** *The randomness of rounding error is independent among nodes and feature dimensions.*

**Assumption 2 (Assumption on loss function)** *The loss function is Lipschitz-smooth and convex.*

Table 1: Statistics of graph datasets. K, M, and B stand for thousand, million, and billion, respectively.

| Datasets | Task | #Graphs | #Avg Nodes | #Avg Edges | #Labels | #Features |
|---|---|---|---|---|---|---|
| Reddit [23] | Node | 1 | 233.0K | 11.6M | 41 | 602 |
| Papers100M [26] | Node | 1 | 111.1M | 1.6B | 172 | 128 |
| MAG240M [26] | Node | 1 | 244.2M | 3.4B | 153 | 768 |
| OGBL-COLLAB [26] | Link | 1 | 235.9K | 1.3M | - | 128 |
| OGBL-PPA [38] | Link | 1 | 576.3K | 30.3M | - | 58 |
| MUTAG [12] | Graph | 188 | 17.9 | 57.5 | 2 | 7 |
| PTC [41] | Graph | 344 | 25.6 | 77.5 | 2 | 19 |
| PROTEINS [7] | Graph | 1113 | 39.1 | 184.7 | 2 | 3 |
| COLLAB [48] | Graph | 5000 | 74.5 | 4989.5 | 3 | 367 |

**Theorem 3** *Given $\epsilon > 0$, $L$-layer GNN with a large enough width $m$. With quantization error satisfy Assumption 1 and loss function satisfy Assumption 2 If we run projected gradient descent for $T$ steps, then with high probability we have*

$$\min_{t=1,\cdots,T}(Loss(W_t, X') - Loss(W_*, X) \leq \epsilon$$

*Remark.* $L(W_*, X)$ is the optimal loss of network trained with original features, and $L(W_t, X')$ is the minimum loss during BiFeat training. So this indicates BiFeat training wouldn't cause much larger loss compared with using original features.

We focus on the difference between GNNs and traditional neural networks. With Assumption1, the aggregation phases help us bound the scale of perturbation caused by quantization. The impact of rounding error to the loss would be negligible as GNN gets deeper.

We are able to quantify this by a key factor $\hat{C}$, decided by graph structure and negatively correlated with the average $L$-hop neighbor number, which would help guide the choice of quantization setup.

The detailed proof of Theorem3 is in Appendix A.

## 5 Evaluation

We run experiments on a multi-GPU server with four NVIDIA Geforce 1080Ti GPUs (11 GB memory for each), 16-core Intel Xeon CPU (2.10 GHz), and 512 GB of RAM. It runs PyTorch [2] and DGL [1]. We train 5 GNN models such as GraphSAGE, GAT, and GIN to fulfill 3 kinds of GNN tasks, namely, node property prediction, link property prediction and graph property regression, over 9 graph datasets. For the heterogeneous graph MAG240M, we transform it into an undirected homogeneous graph and generate features for author and institution nodes by averaging their neighbors' features, which doubles its structure and feature information, in total about 400GB. Table 1 shows the statistics of the datasets.

We use the full-precision training as the natural baseline, denoted by "Full". We also run the two variants of BiFeat, BiFeat-SQ denoted by "SQ" and BiFeat-VQ by "VQ". In addition, we explore the joint effects of enabling PaGraph's caching and quantization methods. We use optimal hyperparameter setup for the full precision baseline. Meanwhile, for each quantized training task, we use the same model setup as "Full" with minor changes in learning rate and dropout probability.

### 5.1 Accuracy Validation

**Node Property Prediction.** To test the accuracy of the node property prediction task, we choose to train four GNN models,GraphSAGE, GAT, ClusterGCN, and MLP, over two datasets, Reddit and OGBN-Papers100M. Though Reddit is a small dataset, it has been widely used as a reference for accuracy validation.

Table 2 summarizes the accuracy results as well as the compression ratios achieved by BiFeat. We draw the following findings. First, across all test cases, SQ achieves a constant compression ratio of 32, as it quantizes each 32 float number of features into an 1-bit integer. Unlike SQ, however, VQ can

Table 2: Node classification accuracy. CR is compression ratio, while Acc is the test set accuracy.

| | | Reddit | | OGBN-Papers100M | |
|---|---|---|---|---|---|
| Model | Method | CR | Acc(%) | CR | Acc(%) |
| GraphSAGE[23] | Full | - | 96.3 | - | 66.1 |
| | SQ | 32 | 96.4 | 32 | 65.4 |
| | VQ | 228.6 | 96.1 | 46.5 | 65.4 |
| GAT[42] | Full | - | 95.3 | - | 65.8 |
| | SQ | 32 | 95.4 | 32 | 64.9 |
| | VQ | 163.2 | 95.3 | 36.6 | 65.3 |
| ClusterGCN[11] | Full | - | 96.0 | - | 63.3 |
| | SQ | 32 | 96.0 | 32 | 62.8 |
| | VQ | 148 | 95.5 | 46.5 | 62.7 |
| MLP[40] | Full | - | 72.6 | - | 46.9 |
| | SQ | 32 | 68.1 | 32 | 35.2 |
| | VQ | 51.2 | 65.1 | 39.4 | 38.1 |

Table 3: Link prediction accuracy

| | | OGBL-PPA | | OGBL-COLLAB | |
|---|---|---|---|---|---|
| Model | Method | CR | Hits@100(%) | CR | Hits@50(%) |
| GCN[24] | Full | - | 18.4 | - | 50.6 |
| | SQ | 32 | 18.5 | 32 | 49.0 |
| | VQ | 46.5 | 18.9 | 46.5 | 49.2 |
| GraphSAGE | Full | - | 16.4 | - | 49.4 |
| | SQ | 32 | 16.3 | 32 | 50.4 |
| | VQ | 46.5 | 16.5 | 46.5 | 49.3 |

achieve significantly higher compression ratios, up to 228.6, while delivering comparable or slightly better accuracy than SQ. Second, compared to the full precision baseline, for models except MLP, both SQ and VQ achieve almost the same accuracy numbers. This implies that shows GNNs usually reach comparable accuracy with aggressive compression. However, MLP observes the maximum accuracy degradation of around 9%, which because of its more sensitive to the input error.

Table 4: Graph classification accuracy

| | | PTC | | MUTAG | | PROTEINS | | COLLAB | |
|---|---|---|---|---|---|---|---|---|---|
| Model | Method | CR | Acc(%) | CR | Acc(%) | CR | Acc(%) | CR | Acc(%) |
| GCN | Full | - | 61.3 | - | 85.6 | - | 74.4 | - | 82.9 |
| | VQ | 152 | 63.4 | 112 | 87.3 | 136 | 74.0 | 1468 | 83.1 |
| GIN[46] | Full | - | 64.1 | - | 87.7 | - | 73.6 | - | 81.8 |
| | VQ | 152 | 65.1 | 112 | 87.8 | 136 | 73.6 | 1468 | 82.2 |

**Link Property Prediction.** Further, we run experiments with link prediction tasks, which are to predict properties of edges (i.e. pairs of nodes). Here, we use two graph datasets, namely, OGBL-PPA and OGBL-COLLAB. OGBL-PPA is a protein-protein association network, organized as an undirected, unweighted graph, with Nodes representing different proteins from 58 species, and edges indicating biologically associations between proteins. OGBL-COLLAB is an author collaboration network, also organized as an undirected graph. We train GCN and GraphSAGE models over these datasets, and report the prediction results in Table 3. Similar to the node property prediction tasks, using both BiFeat-SQ and BiFeat-VQ can achieve comparable link prediction accuracy (Hits@100 in OGBL-PPA, Hits@50 in OGBL-COLLAB) as the full precision baseline. Again, here, BiFeat-VQ shows better compression ratio, which is a constant value 46.5, that is 45% higher than BiFeat-SQ.

**Graph Property Prediction.** As for the graph property prediction tasks, we train GCN and GIN with four datasets PTC, MUTAG, PROTEINS and COLLAB. The first three datasets are bio-informatics datasets, while the last one is a social network dataset. Note that the features of these datasets are

Table 5: Per-epoch time. NC and C stand for settings with caching disabled/enabled

| Model | Method | Reddit | | Papers100M | |
|---|---|---|---|---|---|
| | | NC | C | NC | C |
| Graph-SAGE | Full | 11.60 | 2.47 | 118.5 | 103.1 |
| | SQ | 3.54 | 2.96 | 66.4 | 64.4 |
| | VQ | 3.19 | 2.81 | 69.8 | 67.1 |
| GAT | Full | 13.00 | 3.86 | 195.3 | 187.5 |
| | SQ | 5.28 | 4.49 | 115.3 | 112.2 |
| | VQ | 4.88 | 4.42 | 117.9 | 112.0 |
| Cluster-GCN | Full | 2.23 | 1.68 | 12.91 | 7.24 |
| | SQ | 1.77 | 1.73 | 7.55 | 7.30 |
| | VQ | 1.86 | 1.79 | 8.54 | 7.33 |

Table 6: Accuracy and per-epoch time with MAG240M

| Model | Method | CR | Acc(%) | Epoch time (s) |
|---|---|---|---|---|
| Graph-SAGE | Full | - | 68.6 | 470.9 |
| | SQ | 32 | 68.5 | 114.3 |
| | VQ | 46.5 | 67.7 | 112.2 |
| GAT | Full | - | 67.8 | 509.7 |
| | SQ | 32 | 67.7 | 169.8 |
| | VQ | 46.5 | 67.7 | 163.4 |
| MLP | Full | - | 52.1 | 9.38 |
| | SQ | 32 | 42.0 | 7.07 |
| | VQ | 34.9 | 44.1 | 8.62 |

one-hot encoded, i.e., each feature vector can be represented by a single integer, indicating the index of the only non-zero element in such vector. Clearly, when being applied to such features, our scalar quantization is lossless and behave exactly the same as the full precision baseline. Therefore, we omit its results from Table 4.

On the other hand, since the one-hot codes theoretically have a high lossless compression ratio, to test the accuracy impact of vector quantization while stressing BiFeat, we set a higher compression ratio than the lossless setting. Doing so forces BiFeat-VQ to lose some information during quantization. Table 4 demonstrates that impressively, BiFeat-VQ can actually enhance the training accuracy. Based on our observations, vector quantization extracts the valuable information and filters out noises, thus improving model robustness.

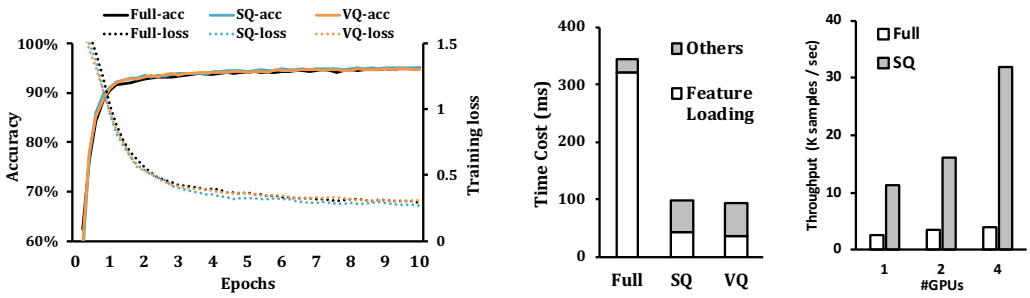
### 5.2 Training Acceleration

Next, we shift our attention from accuracy to the training performance improvement. To this end, we measure the average running time per epoch of node property prediction tasks, where we train three GNN models with both Reddit and OGBN-Papers100M. Here, we additionally compare to another baseline, corresponding to PaGraph's caching, and also explore its joint effects with quantization. In Table 5, with no caching (NC), the two BiFeat quantization variants achieve greatest speedups at 3.27× (SQ) and 3.63× (VQ), for the three models, respectively. When additionally enabling cache, for Reddit, no visible speedups are observed. This is because Reddit can be fully cached into GPU memory, and the two optimizations, caching or quantization, both can completely eliminating data loading. Concerning the Papers100M dataset, two models except ClusterGCN observes speedups of 1.53-1.64×. This is because using cache in full precision features only gets a low speedup due to the proportion of cached node is too low. Feature compression can increase the cache rate and get a high hit rate, allows a higher speedup. Unlike this, combining caching with quantization does not improve performance of the full precision training with caching enabled. This is because the training set of ClusterGCN is relatively small and can be fully cached within GPU memory.

In addition to the per-epoch speedup analysis, we also investigate how the convergence rate evolves as the training runs from epoch to epoch. Here, due to space limit, we choose to train GraphSAGE over Reddit with the full precision baseline and two BiFeat variants, and report the test accuracy results in Figure 3(a). The conclusion drawn here is that using BiFeat, regardless of using SQ or VQ, the quantization-based training can converge to almost the same accuracy without introducing more epochs than the full precision baseline. Together with the above per-epoch performance speedup, we can conclude that BiFeatis able to accelerate the end-to-end training performance of GNNs.

### 5.3 Supporting Giant Graph

Finally, we validate if BiFeatcan accelerate the training of extremely large graphs. Here, we choose MAG240M, the largest graph among our datasets, and run the node property prediction tasks with three models, namely, GraphSAGE, GAT and MLP. We first report the accuracy and per-epoch time results in Table 6. For GraphSAGE and GAT, the two BiFeatvariants achieve comparable accuracy




(a) Loss & Accuracy (b) Breakdown (c) Multi-GPU

Figure 3: Loss and test set accuracy of GraphSAGE training on Reddit with different quantization settings (a); Detailed run time breakdown of GraphSAGE training on MAG240M with different quantization settings (b); Multi-GPU acceleration with GraphSAGE and MAG240M dataset (c)

as the full precision baseline. On the per-epoch time aspect, BiFeat-SQ and BiFeat-VQ introduce speedups of 3.00-4.12x$\times$ and 3.12-4.20$\times$ for the two models, respectively. However, similar to the above results, MLP observes the least benefits of BiFeat, for instance, BiFeatintroduces a maximum accuracy loss of 10%, while only introducing speedups of up to 1.33$\times$.

Second, we conduct the ablation studies to understand the reasons for BiFeat to accelerate the training performance, especially with large graphs. To do so, we measure the changes of the ratio of feature loading across different settings, and summarize the results in Figure 3(b). Within the full precision training, the feature loading is the bottleneck. However, when adopting either SQ or VQ, the feature load time cost has been reduced by up to 90%. We also observe slight increases in the time cost of other tasks, mainly due to the extra dequantization overhead.

Finally, to complement the above single-GPU experiments, here, we run multi-GPU training with MAG240M. As depicted in Figure 3(c), without quantization, adding more GPUs does not necessarily bring performance improvements. This is because the resource contention among training jobs over multiple GPUs exacerbate the feature loading bottleneck. In contrast, using quantization, training performance scales well, due to the reduction in CPU usage and PCIe bandwidth consumption. In the end, we manage to train GraphSAGE over the largest MAG240M dataset using 4 GPUs within one hour, introducing a speedup of up to 8.6$\times$ comparing to the full precision baseline, which has to run over 7.5 hours.

## 6 Conclusion

We pioneer the adoption of the feature quantization methods to break the GPU memory limit and eliminate the feature loading bottleneck, faced by GNN mini-batch training over large graphs. Following this, we materialize our ideas into BiFeat, a GNN feature quantization methodology that supports both Scalar and Vector quantization approaches. Furthermore, we provide theoretical proofs and run extensive experiments to validate that BiFeat can greatly reduce the feature data loading volumes and shorten the end-to-end training time, with bounded accuracy loss.

## References


[1] DGL Homepage. https://www.dgl.ai/. [Online; accessed May-2022].

[2] Pytorch Homepage. https://pytorch.org/. [Online; accessed May-2022].

[3] Alham Fikri Aji and Kenneth Heafield. Sparse communication for distributed gradient descent. arXiv preprint arXiv:1704.05021, 2017.

[4] Zeyuan Allen-Zhu, Yuanzhi Li, and Zhao Song. A convergence theory for deep learning via over-parameterization. In International Conference on Machine Learning, pages 242–252. PMLR, 2019.

[5] Mehdi Bahri, Gaétan Bahl, and Stefanos Zafeiriou. Binary graph neural networks. In Proceedings of the IEEE/CVF Conference on Computer Vision and Pattern Recognition, pages 9492–9501, 2021.

[6] Aleksandar Bojchevski and Stephan Günnemann. Deep gaussian embedding of graphs: Unsupervised inductive learning via ranking. arXiv preprint arXiv:1707.03815, 2017.

[7] Karsten M Borgwardt, Cheng Soon Ong, Stefan Schönauer, SVN Vishwanathan, Alex J Smola, and Hans-Peter Kriegel. Protein function prediction via graph kernels. Bioinformatics, 21(suppl_1):i47–i56, 2005.

[8] Jie Chen, Tengfei Ma, and Cao Xiao. Fastgcn: fast learning with graph convolutional networks via importance sampling. arXiv preprint arXiv:1801.10247, 2018.

[9] Ming Chen, Zhewei Wei, Zengfeng Huang, Bolin Ding, and Yaliang Li. Simple and deep graph convolutional networks. In International Conference on Machine Learning, pages 1725–1735. PMLR, 2020.

[10] Hryhorii Chereda, Annalen Bleckmann, Kerstin Menck, Júlia Perera-Bel, Philip Stegmaier, Florian Auer, Frank Kramer, Andreas Leha, and Tim Beißbarth. Explaining decisions of graph convolutional neural networks: patient-specific molecular subnetworks responsible for metastasis prediction in breast cancer. Genome medicine, 13(1):1–16, 2021.

[11] Wei-Lin Chiang, Xuanqing Liu, Si Si, Yang Li, Samy Bengio, and Cho-Jui Hsieh. Cluster-gcn: An efficient algorithm for training deep and large graph convolutional networks. In Proceedings of the 25th ACM SIGKDD International Conference on Knowledge Discovery & Data Mining, pages 257–266, 2019.

[12] Asim Kumar Debnath, Rosa L Lopez de Compadre, Gargi Debnath, Alan J Shusterman, and Corwin Hansch. Structure-activity relationship of mutagenic aromatic and heteroaromatic nitro compounds. correlation with molecular orbital energies and hydrophobicity. Journal of medicinal chemistry, 34(2):786–797, 1991.

[13] Jacob Devlin, Ming-Wei Chang, Kenton Lee, and Kristina Toutanova. Bert: Pre-training of deep bidirectional transformers for language understanding. arXiv preprint arXiv:1810.04805, 2018.

[14] Mucong Ding, Kezhi Kong, Jingling Li, Chen Zhu, John Dickerson, Furong Huang, and Tom Goldstein. Vq-gnn: A universal framework to scale up graph neural networks using vector quantization. Advances in Neural Information Processing Systems, 34, 2021.

[15] Jialin Dong, Da Zheng, Lin F Yang, and Geroge Karypis. Global neighbor sampling for mixed cpu-gpu training on giant graphs. arXiv preprint arXiv:2106.06150, 2021.

[16] Boyuan Feng, Yuke Wang, Xu Li, Shu Yang, Xueqiao Peng, and Yufei Ding. Sgquant: Squeezing the last bit on graph neural networks with specialized quantization. In 2020 IEEE 32nd International Conference on Tools with Artificial Intelligence (ICTAI), pages 1044–1052. IEEE, 2020.

[17] Matthias Fey, Jan E Lenssen, Frank Weichert, and Jure Leskovec. Gnnautoscale: Scalable and expressive graph neural networks via historical embeddings. In International Conference on Machine Learning, pages 3294–3304. PMLR, 2021.

[18] Matthias Fey and Jan Eric Lenssen. Fast graph representation learning with pytorch geometric. arXiv preprint arXiv:1903.02428, 2019.

[19] Ruiqi Gao, Tianle Cai, Haochuan Li, Cho-Jui Hsieh, Liwei Wang, and Jason D Lee. Convergence of adversarial training in overparametrized neural networks. Advances in Neural Information Processing Systems, 32, 2019.

[20] Allen Gersho and Robert M Gray. Vector quantization and signal compression, volume 159. Springer Science & Business Media, 2012.

[21] Robert Gray. Vector quantization. IEEE Assp Magazine, 1(2):4–29, 1984.

[22] Paul Haase, Heiko Schwarz, Heiner Kirchhoffer, Simon Wiedemann, Talmaj Marinc, Arturo Marban, Karsten Müller, Wojciech Samek, Detlev Marpe, and Thomas Wiegand. Dependent scalar quantization for neural network compression. In 2020 IEEE International Conference on Image Processing (ICIP), pages 36–40. IEEE, 2020.

[23] Will Hamilton, Zhitao Ying, and Jure Leskovec. Inductive representation learning on large graphs. Advances in neural information processing systems, 30, 2017.

[24] Negar Heidari and Alexandros Iosifidis. Progressive graph convolutional networks for semi-supervised node classification. IEEE Access, 9:81957–81968, 2021.

[25] Jared Heinly, Enrique Dunn, and Jan-Michael Frahm. Comparative evaluation of binary features. In European Conference on Computer Vision, pages 759–773. Springer, 2012.

[26] Weihua Hu, Matthias Fey, Marinka Zitnik, Yuxiao Dong, Hongyu Ren, Bowen Liu, Michele Catasta, and Jure Leskovec. Open graph benchmark: Datasets for machine learning on graphs. Advances in neural information processing systems, 33:22118–22133, 2020.

[27] Ziniu Hu, Yuxiao Dong, Kuansan Wang, Kai-Wei Chang, and Yizhou Sun. Gpt-gnn: Generative pre-training of graph neural networks. In Proceedings of the 26th ACM SIGKDD International Conference on Knowledge Discovery & Data Mining, pages 1857–1867, 2020.

[28] Itay Hubara, Matthieu Courbariaux, Daniel Soudry, Ran El-Yaniv, and Yoshua Bengio. Binarized neural networks. In Proceedings of the 30th International Conference on Neural Information Processing Systems, NIPS'16, page 4114–4122, Red Hook, NY, USA, 2016. Curran Associates Inc.

[29] Thomas N Kipf and Max Welling. Semi-supervised classification with graph convolutional networks. arXiv preprint arXiv:1609.02907, 2016.

[30] Yujun Lin, Song Han, Huizi Mao, Yu Wang, and William J Dally. Deep gradient compression: Reducing the communication bandwidth for distributed training. arXiv preprint arXiv:1712.01887, 2017.

[31] Zhiqi Lin, Cheng Li, Youshan Miao, Yunxin Liu, and Yinlong Xu. Pagraph: Scaling gnn training on large graphs via computation-aware caching. In Proceedings of the 11th ACM Symposium on Cloud Computing, pages 401–415, 2020.

[32] Meng Liu, Hongyang Gao, and Shuiwang Ji. Towards deeper graph neural networks. In Proceedings of the 26th ACM SIGKDD international conference on knowledge discovery & data mining, pages 338–348, 2020.

[33] Zechun Liu, Wenhan Luo, Baoyuan Wu, Xin Yang, Wei Liu, and Kwang-Ting Cheng. Bi-real net: Binarizing deep network towards real-network performance. Int. J. Comput. Vision, 128(1):202–219, jan 2020.

[34] Pau Rodríguez, Miguel A Bautista, Jordi Gonzàlez, and Sergio Escalera. Beyond one-hot encoding: Lower dimensional target embedding. Image and Vision Computing, 75:21–31, 2018.

[35] Frank Seide, Hao Fu, Jasha Droppo, Gang Li, and Dong Yu. 1-bit stochastic gradient descent and its application to data-parallel distributed training of speech dnns. In Fifteenth Annual Conference of the International Speech Communication Association, 2014.

[36] John E Stone, David J Hardy, Ivan S Ufimtsev, and Klaus Schulten. Gpu-accelerated molecular modeling coming of age. Journal of Molecular Graphics and Modelling, 29(2):116–125, 2010.

[37] Nikko Strom. Scalable distributed dnn training using commodity gpu cloud computing. In Proceedings of Sixteenth Annual Conference of the International Speech Communication Association, 2015.

[38] Damian Szklarczyk, Annika L Gable, David Lyon, Alexander Junge, Stefan Wyder, Jaime Huerta-Cepas, Milan Simonovic, Nadezhda T Doncheva, John H Morris, Peer Bork, et al. String v11: protein–protein association networks with increased coverage, supporting functional discovery in genome-wide experimental datasets. Nucleic acids research, 47(D1):D607–D613, 2019.

[39] Shyam A Tailor, Javier Fernandez-Marques, and Nicholas D Lane. Degree-quant: Quantization-aware training for graph neural networks. arXiv preprint arXiv:2008.05000, 2020.

[40] Hind Taud and JF Mas. Multilayer perceptron (mlp). In Geomatic approaches for modeling land change scenarios, pages 451–455. Springer, 2018.

[41] Hannu Toivonen, Ashwin Srinivasan, Ross D King, Stefan Kramer, and Christoph Helma. Statistical evaluation of the predictive toxicology challenge 2000–2001. Bioinformatics, 19(10):1183–1193, 2003.

[42] Petar Veličković, Guillem Cucurull, Arantxa Casanova, Adriana Romero, Pietro Lio, and Yoshua Bengio. Graph attention networks. arXiv preprint arXiv:1710.10903, 2017.

[43] Minjie Wang, Da Zheng, Zihao Ye, Quan Gan, Mufei Li, Xiang Song, Jinjing Zhou, Chao Ma, Lingfan Yu, Yu Gai, et al. Deep graph library: A graph-centric, highly-performant package for graph neural networks. arXiv preprint arXiv:1909.01315, 2019.

[44] Wei Wen, Cong Xu, Feng Yan, Chunpeng Wu, Yandan Wang, Yiran Chen, and Hai Li. Terngrad: Ternary gradients to reduce communication in distributed deep learning. In Proceedings of Advances in neural information processing systems, pages 1509–1519, 2017.

[45] Yongji Wu, Defu Lian, Yiheng Xu, Le Wu, and Enhong Chen. Graph convolutional networks with markov random field reasoning for social spammer detection. In Proceedings of the AAAI Conference on Artificial Intelligence, volume 34, pages 1054–1061, 2020.

[46] Keyulu Xu, Weihua Hu, Jure Leskovec, and Stefanie Jegelka. How powerful are graph neural networks? In International Conference on Learning Representations, 2019.

[47] Kun Xu, Liwei Wang, Mo Yu, Yansong Feng, Yan Song, Zhiguo Wang, and Dong Yu. Cross-lingual knowledge graph alignment via graph matching neural network. arXiv preprint arXiv:1905.11605, 2019.

[48] Pinar Yanardag and SVN Vishwanathan. A structural smoothing framework for robust graph comparison. Advances in neural information processing systems, 28, 2015.

Table 7: Summary of notations.

| Notation | Description |
|---|---|
| $n$ | Number of nodes in the graph. |
| $d$ | Input features dimension. |
| $m$ | Hidden layer dimension, also known as the width of network. |
| $N(i)$ | Set of nodes adjacent to $i$. |
| $L$ | Number of layers. |
| $[n]$ | $\{1, 2, \cdots, n\}$. |
| $\boldsymbol{X}$ | Input features of all nodes, with shape $n \times d$. Note that we also use $x_i$ to denote features of node $i$. |
| $\boldsymbol{X}'$ | Quantized input features of all nodes with the same shape as $\boldsymbol{X}$. |
| $\boldsymbol{A}$ | Input layer weights with the shape of $m \times d$. |
| $\boldsymbol{W}$ | Hidden layer weights $\boldsymbol{W} = (\boldsymbol{W}_1, \cdots, \boldsymbol{W}_L)$, where weights of each layer has the shape of $m \times d$. |
| $a$ | Output layer weights with the shape of $m \times 1$. |
| $\boldsymbol{D}$ | Diagonal matrix, $\boldsymbol{D}_{i,l} = diag(I(\overline{g}_{i,l} \geq 0))$, where $I$ is the element-wise indicator function. |
| $f_i(\boldsymbol{W}, \boldsymbol{X})$ | Output of node $i$ with weights $\boldsymbol{W}$ and input $\boldsymbol{X}$ |
| $l$ | Loss function |
| $Loss(\boldsymbol{W}, \boldsymbol{X})$ | Loss with weights $\boldsymbol{W}$ and inputs $\boldsymbol{X}$ |
| $B(R)$ | The neighborhood of initial weights, $B(R) = \{\boldsymbol{W} : \|\boldsymbol{W}_l - \boldsymbol{W}_l^{(0)}\|_F \leq R/\sqrt{m}, l \in [L]\}$ |
| $\mathcal{P}_{B(R)}$ | Euclidean projection to the convex set $B(R)$. |
| $\alpha$ | Step size of projected gradient descent. |
| $T$ | Number of steps. |
| $C_{i,l}^f$ | The expected scale of node $i$'s features after the aggregation of $l$ layers. |
| $C_{i,l}^e$ | The expected scale of node $i$'s error caused by quantization after the aggregation of $l$ layers. |
| $\overline{C}_L^f$ | The mean value of $C_{i,L}^f$. |
| $\overline{C}_L^e$ | The mean value of $C_{i,L}^e$. |
| $\hat{C}_L$ | $C_{i,L}^e / C_{i,L}^f$. |

# A Proof of Theorem 3

We organize the proof as follows. First, we formally define the structure of graph neural network (GNN) in Section A.1. Then we give the detailed proof throughout Section A.2- A.4: (1) we prove that the gradient is bounded and the loss function is almost convex within the neighborhood of random initialization in Section A.2; (2) we prove that with the optimal weights of uncompressed features, quantized features produce a bounded loss compared to the uncompressed features in Section A.3; and (3) with the help of the lemmas introduced in (1) and (2), we prove Theorem 3 in Section A.4. Finally, we present an analysis of the factors that may affect the compression ratio in Section A.5.

## A.1 GNN Definitions

As Graph Convolutional Network (GCN) is one of the most widely-used GNN models, we use it to drive our theoretical proofs and analysis. Here, we follow the literature [29] to define the GCN structure as follows:

$$
\begin{aligned}
&g_{i,0} = \boldsymbol{A}x_i \\
&h_{i,0} = \phi(g_{i,0}) \\
&g_{i,l} = \boldsymbol{W}_l h_{i,l-1} && , for\ i \in [n]\ and\ l \in [L] \\
&\overline{g}_{i,l} = \textstyle\sum_{j \in N(i)} \frac{1}{|N(i)|} g_{j,l} && , for\ i \in [n]\ and\ l \in [L] \\
&h_{i,l} = \phi(\overline{g}_{i,l}) && , for\ i \in [n]\ and\ l \in [L] \\
&f_i(W, X) = a^\top h_{i,L}
\end{aligned}
$$

Here $x_i$ is the input feature, $g_{i,l}$ and $h_{i,l}$ are the feature vectors of node $i$ before and after the ReLU activation function $\phi$ of layer $l$. Note that these notations and definitions are similar with

those traditional DNN architecture studied in [19, 4]. However, the main difference lies in that GNN introduces an aggregation phase i.e. $\overline{g}_{i,l}$, where it gathers information by averaging neighbor features. It can also be written in a GCN style as $\overline{g}_{i,l} = \boldsymbol{G}_l \boldsymbol{L}_{:,i}$, where $\boldsymbol{G}_l = (g_{1,l}, \cdots, g_{n,l})$. We set $\boldsymbol{L} = \hat{\boldsymbol{D}}^{-1}\hat{\boldsymbol{A}}$, where $\hat{\boldsymbol{A}}$ and $\hat{\boldsymbol{D}}$ are the adjacency matrix and degree matrix including self loop. We use the diagonal matrix $\boldsymbol{D}$ to indicate the consequences of ReLU function, so $h_{i,l}$ can be written as $\boldsymbol{D}_{i,l}\overline{g}_{i,l}$.

With $\boldsymbol{S} = \{x \in \mathbb{R}^d : \|x\|_2 = 1\}$, we scale the input features to $\boldsymbol{X} = \{x_i \in \boldsymbol{S} : i \in [n]\}$ following [4]. We also follow the same initialization method as Definition 2.3 in [4] with a minor change on the output layer: $a_j \sim \mathcal{N}(0, 1/\overline{C}_L^f)$. This is intended to ensure the output scale fits the label, $\overline{C}_L^f$ is a factor we discuss in Section A.5. We only train hidden layer weights $\boldsymbol{W}$ while keeping input and output layer weights $\boldsymbol{A}$ and $a$ with random initialization as [4] does.

We denote $\mathcal{P}_{B(R)}$ as the Euclidean projection to the convex set $B(R)$ and $\boldsymbol{W}^{(t)}$ as the Weights after $t$ iterations. We run projected gradient descent based on the constraint set $B(R)$ with step size $\alpha$ for $T$ steps using the following update rule.

$$\begin{aligned}\boldsymbol{V}^{(t+1)} &= \boldsymbol{W}^{(t)} - \alpha \nabla_{\boldsymbol{W}} Loss(\boldsymbol{W}^{(t)}, \boldsymbol{X}),\\ \boldsymbol{W}^{(t+1)} &= \mathcal{P}_{B(R)}(\boldsymbol{V}^{(t+1)})\end{aligned}$$

To measure the effect of aggregation, we introduce two factors $C_{i,l}^e$ and $C_{i,l}^f$ to represent the expectation of scaling of $h_{i,l}$ caused by the aggregation of $l$ layers. These factors have the following properties:

$$C_{i,0}^e = 1, \quad C_{i,0}^f = 1$$

$$C_{i,l+1}^e = \sqrt{\sum_{j\in N(i)}\sum_{k\in N(i)} r_{l,j,k}^e \frac{1}{|N(i)|^2} C_{j,l}^e C_{k,l}^e}, \quad C_{i,l+1}^f = \sqrt{\sum_{j\in N(i)}\sum_{k\in N(i)} r_{l,j,k}^f \frac{1}{|N(i)|^2} C_{j,l}^f C_{k,l}^f}$$

$$C_{i,l}^e \le 1, \quad C_{i,l}^f \le 1$$

where $r_{l,j,k}^f$ and $r_{l,j,k}^e$ denotes the correlation of feature components and errors in layer $l$ between the node $j$ and node $k$, respectively. With Assumption 1, $r_{0,j,k}^e = 0$ $(j \neq k)$, $C_{i,l}^e$ is determined by the graph structure. $C_{i,l}^f$ is also relative to the graph structure, but it is also affected by the correlation of node features. $C_{i,l}^e \le C_{i,l}^f$ has a high probability as $r_{0,j,k}^f > 0$ has high probability. So we have $\frac{C_{i,l}^e}{C_{i,l}^f} \le 1$. $C_{i,l}^e$ and $C_{i,l}^f$ can also be seen as weighted average of $l$-hop neighbors, thus we have $C_{i,l}^e \ge \frac{1}{n}$ and $C_{i,l}^f \ge \frac{1}{n}$. Therefore, we expect the value of $C_{i,l}^e$ , $C_{i,l}^f$, and $C_{i,l}^e$ / $C_{i,l}^f$ gets smaller as the layer $l$ gets deeper. While the exact value of these factors could not be directly calculated with the statistics of graph, we can obtain them through quick profiling tests and derive the bound from the analysis. We conduct an analysis of these factors in Section A.5.

### A.2 Gradient Bounds and Almost Convex

In this subsection, we will prove that the gradient is bounded and the loss function is almost convex with regard to weights within the neighborhood of random initialization. We use the same proof sketch as [19], but our proof differs by having fixed input features.

**Lemma 4** *If $m \ge d$, with probability $1 - O(nL)e^{-\Omega(m)}$ at initialization, we have $\|\boldsymbol{A}\|_2 = O(1)$, $\|\boldsymbol{W}_L\|_2 = O(1), \forall l \in [L]$, and $\|a\|_2 = O(\frac{\sqrt{m}}{\overline{C}_L^f})$.*

**Lemma 5** *For any fixed input $\boldsymbol{X} = \{x_i \in \boldsymbol{S} : i \in [n]\}$, with probability $1 - O(L)e^{-\Omega(m/L)}$ over the randomness of initialization, we have $\forall i \in [n]$ and $l \in \{0, ..., L\}$, $\|h_{i,l}\|_2 \in [\frac{2}{3}C_{i,l}^f, \frac{4}{3}C_{i,l}^f]$.*

**Lemma 6** *If $m = \Omega(LlogL)$, for any fixed input $\boldsymbol{X} = \{x_i \in \boldsymbol{S} : i \in [n]\}$ , with probability $1 - e^{-\Omega(m/L)}$ over the randomness of initialization, we have for every $l \in [L]$ and every $i \in [n]$,$\|a^\top \boldsymbol{D}_{i,L}\boldsymbol{W}_{i,L} \cdots \boldsymbol{D}_{i,l}\boldsymbol{W}_{i,l}\|_2 = O(\frac{\sqrt{mL}}{\overline{C}_L^f})$.*

*Proof of lemma4, lemma5, lemma6.* These are restatements of Lemma A.1, Lemma A.2 and Lemma A.3 in [19]. Since our GNN architecture shares the same weight initialization method as regular DNN, we can directly apply these results over the randomness of initialization. In Lemma 5 the value is different from Lemma A.2 in [19] due to aggregation, but with the same random weight initialization, the probability and relative bound is consistent.

We prove the perturbation of gradients caused by perturbation of weights is small following [4].

**Lemma 7** *Given any fixed inputs $\boldsymbol{X} = \{x_i \in \boldsymbol{S} : i \in [n]\}$. If $m \geq max(d, \Omega(LlogL))$, $\frac{R}{\sqrt{m}} \leq \frac{1}{SL^6(\log m)^3}$ for some sufficiently large constant S, with probability $1 - O(L)e^{-\Omega((mR)^{2/3}L)}$ over the randomness of initialization, we have for any $\boldsymbol{W} \in B(R)$ , any $l \in [L]$ and every $i \in [n]$,*

$$\|\frac{\partial f_i(\boldsymbol{W}, X)}{\partial \boldsymbol{W}_l} - \frac{\partial f_i(\boldsymbol{W}^{(0)}, X)}{\partial \boldsymbol{W}_l}\|_F = O(\frac{R^{1/3}m^{1/3}L^2\sqrt{\log m}}{\overline{C}_L^f}),$$

$$\|\frac{\partial f_i(\boldsymbol{W}, X)}{\partial \boldsymbol{W}_l}\|_F = O(\frac{\sqrt{mL}}{\overline{C}_L^f})$$

*Proof.* We denote $\boldsymbol{D}'$, $\boldsymbol{W}'$, and $h'$ as perturbed $\boldsymbol{D}$, $\boldsymbol{W}$, and $h$, respectively. With Claim 8.3 and Lemma 8.2(c) of [4], we have that when $\frac{R}{\sqrt{m}} \leq \frac{1}{SL^6(\log m)^3}$, with probability $1 - e^{-\Omega(m(R/\sqrt{m})^{2/3}L)}$,

$$\|\boldsymbol{D}'_{i,l} - \boldsymbol{D}_{i,l}\|_0 = O(m(\frac{R}{\sqrt{m}})^{2/3}L) \tag{3}$$

and

$$\|h'_{i,l} - h_{i,l}\|_0 = O(C_{i,l}^f \frac{R}{\sqrt{m}} L^{5/2}\sqrt{\log m}) \tag{4}$$

Combining (3) and Lemma 8.7 of [4], we get:

$$\begin{aligned}&\|(a^\top \boldsymbol{D}'_{i,L}\boldsymbol{W}'_L \cdots \boldsymbol{D}'_{i_{l+1},l+1}\boldsymbol{W}'_{l+1}\boldsymbol{D}'_{i_L,l}) - (a^\top \boldsymbol{D}_{i,L}\boldsymbol{W}_L \cdots \boldsymbol{D}_{i_{l+1},l+1}\boldsymbol{W}_{l+1}\boldsymbol{D}_{i_L,l})\|_2 \\ &\leq O(\frac{1}{\overline{C}_L^f}(\frac{R}{\sqrt{m}})^{1/3}L^2\sqrt{m\log m})\end{aligned}$$

During backward propagation, we have:

$$\frac{\partial f_i(\boldsymbol{W}, X)}{\partial \boldsymbol{W}_L} = \underbrace{\sum_{i_{L-1}\in N(i)} \frac{1}{|N(i)|} \cdots \sum_{i_L \in N(i_{l+1})} \frac{1}{|N(i_{l+1})|}}_{L-l \ sums} h_{i_L,l-1} a^\top \boldsymbol{D}_{i,L}\boldsymbol{W}_L \cdots \boldsymbol{D}_{i_{l+1},l+1}\boldsymbol{W}_{l+1}\boldsymbol{D}_{i_L,l}$$

Then, using Lemma5, Lemma6, and the above results, we have:

$$\|\frac{\partial f_i(\boldsymbol{W},X)}{\partial \boldsymbol{W}_l}-\frac{\partial f_i(\boldsymbol{W}^{(0)},X)}{\partial \boldsymbol{W}_l}\|_F=\|\underbrace{\sum_{i_{L-1}\in N(i)}\frac{1}{|N(i)|}\cdots\sum_{i_L\in N(i_{l+1})}\frac{1}{|N(i_{l+1})|}}_{L-l\ sums}$$

$$h'_{i_L,l-1}a^\top \boldsymbol{D}'_{i,L}\boldsymbol{W}'_L\cdots\boldsymbol{D}'_{i_{l+1},l+1}\boldsymbol{W}'_{l+1}\boldsymbol{D}'_{i_L,l}-h_{i_L,l-1}a^\top \boldsymbol{D}_{i,L}\boldsymbol{W}_L\cdots\boldsymbol{D}_{i_{l+1},l+1}\boldsymbol{W}_{l+1}\boldsymbol{D}_{i_L,l}\|_F$$

$$\leq\underbrace{\sum_{i_{L-1}\in N(i)}\frac{1}{|N(i)|}\cdots\sum_{i_L\in N(i_{l+1})}\frac{1}{|N(i_{l+1})|}}_{L-l\ sums}[\|h'_{i_L,l-1}-h_{i_L,l-1}\|_2\cdot\|a^\top \boldsymbol{D}_{i,L}\boldsymbol{W}_L\cdots\boldsymbol{W}_{l+1}\boldsymbol{D}_{i_L,l}\|_2$$

$$+\|h_{i_L,l-1}\|_2\cdot\|(a^\top \boldsymbol{D}'_{i,L}\boldsymbol{W}'_L\cdots\boldsymbol{W}'_{l+1}\boldsymbol{D}'_{i_L,l})-(a^\top \boldsymbol{D}_{i,L}\boldsymbol{W}_L\cdots\boldsymbol{W}_{l+1}\boldsymbol{D}_{i_L,l})\|_2$$

$$\leq\underbrace{\sum_{i_{L-1}\in N(i)}\frac{1}{|N(i)|}\cdots\sum_{i_L\in N(i_{l+1})}\frac{1}{|N(i_{l+1})|}}_{L-l\ sums}[O(C^f_{i,l-1}\frac{R}{\sqrt{m}}L^{5/2}\sqrt{\log m})\cdot O(\frac{\sqrt{mL}}{\overline{C}^f_L})$$

$$+O(C^f_{i,l-1})\cdot O(\frac{1}{\overline{C}^f_L}(\frac{R}{\sqrt{m}})^{1/3}L^2\sqrt{m\log m})]$$

$$=\underbrace{\sum_{i_{L-1}\in N(i)}\frac{1}{|N(i)|}\cdots\sum_{i_L\in N(i_{l+1})}\frac{1}{|N(i_{l+1})|}}_{L-l\ sums}O(\frac{C^f_{i,l-1}}{\overline{C}^f_L}R^{1/3}m^{1/3}L^2\sqrt{\log m})$$

$$=O(\frac{R^{1/3}m^{1/3}L^2\sqrt{\log m}}{\overline{C}^f_L})$$

where $C^f_{i,l-1}\leq 1$.

With Lemma5, Lemma6, (4), and $\frac{R}{\sqrt{m}}\leq\frac{1}{SL^6(\log m)^3}$, we have

$$\|\frac{\partial f_i(\boldsymbol{W},X)}{\partial \boldsymbol{W}_l}\|_F=O(\frac{\sqrt{mL}}{\overline{C}^f_L})\cdot(O(C^f_{i,l})+O(C^f_{i,l}\frac{R}{\sqrt{m}}L^{5/2}\sqrt{\log m}))=O(\frac{C^f_{i,l}\sqrt{mL}}{\overline{C}^f_L})=O(\frac{\sqrt{mL}}{\overline{C}^f_L})$$

Then we are able to prove the loss function is almost convex within the neighborhood $B(R)$ for any fixed $X$.

**Lemma 8** *If $R=O(\frac{\sqrt{m}}{L^6(\log m)^3})$, with probability at least $1-O(nL)e^{-\Omega((mR)^{2/3}L)}$ over random initialization, we have for any $\boldsymbol{W}^{(1)},\boldsymbol{W}^{(2)}\in B(R)$, any $\boldsymbol{X}=\{x_i\in\boldsymbol{S}:i\in[n]\}$, and any $Y=(y_1,\cdots,y_n)\in\mathbb{R}^n$,*

$$l(f_i(\boldsymbol{W}^{(2)},X),y_i)\geq l(f_i(\boldsymbol{W}^{(1)},X),y_i)+\left\langle\nabla_{\boldsymbol{W}}l(f_i(\boldsymbol{W},X),y_i),\boldsymbol{W}^{(2)}-\boldsymbol{W}^{(1)}\right\rangle$$
$$-\|\boldsymbol{W}^{(2)}-\boldsymbol{W}^{(1)}\|_F O(\frac{R^{1/3}m^{1/3}L^{5/2}\sqrt{\log m}}{\overline{C}^f_L})$$

*Proof.* For any fixed $X$ and any fixed $i$, with probability $1-O(nL)e^{-\Omega((mR)^{2/3}L)}$, we have:

$$l(f_i(\boldsymbol{W}^{(2)},X),y_i)-l(f_i(\boldsymbol{W}^{(1)},X),y_i)-\left\langle\nabla_{\boldsymbol{W}}l(f_i(\boldsymbol{W},X),y_i),\boldsymbol{W}^{(2)}-\boldsymbol{W}^{(1)}\right\rangle$$

$$\geq\frac{\partial}{\partial f}l(f_i(\boldsymbol{W}^{(1)},X),y_i)[f_i(\boldsymbol{W}^{(2)},X)-f_i(\boldsymbol{W}^{(1)},X)-\left\langle\nabla_{\boldsymbol{W}}f_i(\boldsymbol{W}^{(1)},X),\boldsymbol{W}^{(2)}-\boldsymbol{W}^{(1)}\right\rangle]$$

$$=\frac{\partial}{\partial f}l(f_i(\boldsymbol{W}^{(1)},X),y_i)\left\langle\int_0^1(\nabla_{\boldsymbol{W}}f_i(t\boldsymbol{W}^{(2)}+(1-t)\boldsymbol{W}^{(1)},X)-\nabla_{\boldsymbol{W}}f_i(\boldsymbol{W}^{(1)},X))dt,\boldsymbol{W}^{(2)}-\boldsymbol{W}^{(1)}\right\rangle$$

$$\geq-\|\boldsymbol{W}^{(2)}-\boldsymbol{W}^{(1)}\|_F O(\frac{R^{1/3}m^{1/3}L^{5/2}\sqrt{\log m}}{\overline{C}^f_L})$$

The first inequality is due to convexity of $l$ with regard to $f$ and the second inequality is due to Lemma 7. $\frac{\partial l}{\partial f}$ is bounded and $\frac{\partial f}{\partial \boldsymbol{W}} = (\frac{\partial f}{\partial \boldsymbol{W}_1}, \cdots, \frac{\partial f}{\partial \boldsymbol{W}_L})$.

### A.3 Loss after Quantization

In this subsection we prove with the optimal weights of uncompressed features, the difference between losses using quantized features and original features as input is small.

**Lemma 9** *Let $\boldsymbol{W}^{(*)} = \arg\min_{\boldsymbol{W} \in B(R)} Loss(\boldsymbol{W}, X)$ be the optimal weights of GNN trained using original features $X$, with loss function satisfying Assumption2, use the same weights on quantized features $X'$ satisfying $\|x_i' - x_i\|_2 \leq \delta$ and Assumption 1, with high probability over the randomness of initialization of $a^\top$ we have*

$$Loss(\boldsymbol{W}^{(*)}, X') - Loss(\boldsymbol{W}^{(*)}, X) = O(\hat{C}_L \delta)$$

*Proof.* We denote $\boldsymbol{W}^{(*)}$ as the optimal weights without feature compression, so the optimal loss is $Loss(\boldsymbol{W}^{(*)}, X)$. We use $h_{i,l}(X)$ to indicate $h_{i,l}$ with regard to input feature $X$, we can get

$$\begin{aligned}
Loss(\boldsymbol{W}^{(*)}, X') - Loss(\boldsymbol{W}^{(*)}, X) =& \frac{1}{n}\sum_{i=1}^{n}[l(f_i(\boldsymbol{W}^{(*)}, X'), y_i) - l(f_i(\boldsymbol{W}^{(*)}, X), y_i)] \\
=& \frac{1}{n}\sum_{i=1}^{n}\frac{\partial l}{\partial f}(f_i(\boldsymbol{W}^{(*)}, X') - f_i(\boldsymbol{W}^{(*)}, X)) \\
=& \frac{1}{n}\sum_{i=1}^{n}\frac{\partial l}{\partial f}(a^\top(h_{i,L}(X') - h_{i,L}(X))) \\
=& \frac{1}{n}\sum_{i=1}^{n} O(\frac{1}{\overline{C}_L^f}) \cdot O(\delta C_{i,L}^e) \\
=& O(\frac{\delta \overline{C}_L^e}{\overline{C}_L^f}) \\
=& O(\hat{C}_L \delta)
\end{aligned}$$

where we define $\hat{C}_L = \frac{\overline{C}_L^e}{\overline{C}_L^f}$.

### A.4 Proof of Theorem3

With Lemma7, Lemma8, and Lemma9, we are ready to prove Theorem3.

*Proof of Theorem3.* For a projected gradient descent with in total $T$ steps starting from initialization $\boldsymbol{W}^{(0)}$, we denote $\boldsymbol{W}^{(t)}$ as the weights after $t$ steps with step size $\alpha$. $\boldsymbol{W}^{(t)} \in B(R)$ holds for all $t = 0, 1, \cdots, T$.

The update rule of projected gradient descent is $\boldsymbol{W}^{(t+1)} = \mathcal{P}_{B(R)}(\boldsymbol{V}^{(t+1)})$, $\boldsymbol{V}^{(t+1)} = \boldsymbol{W}^{(t)} - \alpha \nabla_{\boldsymbol{W}} Loss(\boldsymbol{W}^{(t)})$. Let $d_t = \|\boldsymbol{W}^{(t)} - \boldsymbol{W}^{(*)}\|_F$. If $R = O(\frac{\sqrt{m}}{L^6 (\log m)^3})$ and loss function satisfies

Assumption2, with probability at least $1 - O(nL)e^{-\Omega((mR)^{2/3}L)}$ over random initialization, we have

$$
\begin{aligned}
d_{t+1}^2 =& \|\boldsymbol{W}^{(t+1)} - \boldsymbol{W}^{(*)}\|_F^2 \\
\leq& \|\boldsymbol{V}^{(t+1)} - \boldsymbol{W}^{(*)}\|_F^2 \\
=& \|\boldsymbol{W}^{(t)} - \boldsymbol{W}^{(*)}\|_F^2 + 2\left\langle V_{t+1} - \boldsymbol{W}^{(t)}, \boldsymbol{W}^{(t)} - \boldsymbol{W}^{(*)} \right\rangle + \|V_{t+1} - \boldsymbol{W}^{(t)}\|_F^2 \\
=& d_t^2 + 2\alpha \left\langle \nabla_{\boldsymbol{W}} L'(\boldsymbol{W}^{(t)}), \boldsymbol{W}^{(*)} - \boldsymbol{W}^{(t)} \right\rangle + \alpha^2 \|\nabla_{\boldsymbol{W}} L'(\boldsymbol{W}^{(t)})\|_F^2 \\
=& d_t^2 + \frac{2\alpha}{n} \sum_{i=1}^{n} \left\langle \nabla_{\boldsymbol{W}} l(f_i(\boldsymbol{W}^{(t)}, X'), y_i), \boldsymbol{W}^{(*)} - \boldsymbol{W}^{(t)} \right\rangle + \alpha^2 \| \frac{1}{n} \sum_{i=1}^{n} \frac{\partial l}{\partial f} \nabla_{\boldsymbol{W}} f_i(\boldsymbol{W}^{(t)}, X')\|_F^2 \\
\leq& d_t^2 + \frac{2\alpha}{n} \sum_{i=1}^{n} [l(f_i(\boldsymbol{W}^{(*)}, X'), y_i) - l(f_i(\boldsymbol{W}^{(t)}, X'), y_i) + \\
& \|\boldsymbol{W}^{(*)} - \boldsymbol{W}^{(t)}\|_F O(\frac{R^{1/3} m^{1/3} L^{5/2} \sqrt{\log m}}{\overline{C}_L^f})] + \alpha^2 O(\frac{mL^2}{(\overline{C}_L^f)^2}) \\
\leq& d_t^2 + 2\alpha [Loss(\boldsymbol{W}^{(*)}, X) + O(\hat{C}_L \delta) - Loss(\boldsymbol{W}^{(t)}, X')] + \\
& O(\alpha \frac{R^{4/3} m^{-1/6} L^{5/2} \sqrt{\log m}}{\overline{C}_L^f} + \alpha^2 \frac{mL^2}{(\overline{C}_L^f)^2}) \\
\leq& d_t^2 + 2\alpha [Loss(\boldsymbol{W}^{(*)}, X) - Loss(\boldsymbol{W}^{(t)}, X')] + O(\alpha \frac{R^{4/3} m^{-1/6} L^{5/2} \sqrt{\log m}}{\overline{C}_L^f} + \alpha^2 \frac{mL^2}{(\overline{C}_L^f)^2} + \alpha \hat{C}_L \delta)
\end{aligned}
$$

where the second inequality is for Lemma8 and Lemma7, the third inequality is due to Lemma9. Note that Lemma8 and Lemma7 can be satisfied with $m = max(\Omega(\frac{L^{16} R^9}{(\overline{C}_L^f)^7 \epsilon^7}), \Omega(d^2))$.

Using induction, we have

$$
\begin{aligned}
d_T^2 \leq& d_0^2 + 2\alpha \sum_{t=0}^{T+1} [Loss(\boldsymbol{W}^{(*)}, X) - Loss(\boldsymbol{W}^{(t)}, X')] + \\
& O(T(\alpha \frac{R^{4/3} m^{-1/6} L^{5/2} \sqrt{\log m}}{\overline{C}_L^f} + \alpha^2 \frac{mL^2}{(\overline{C}_L^f)^2} + \alpha \hat{C}_L \delta))
\end{aligned}
$$

which implies that

$$
\begin{aligned}
\min_{0 \leq t \leq T} (Loss(\boldsymbol{W}^{(t)}, X') - Loss(\boldsymbol{W}^{(*)}, X)) \leq& \frac{d_0^2 - d_T^2}{\alpha T} + O(\frac{R^{4/3} m^{-1/6} L^{5/2} \sqrt{\log m}}{\overline{C}_L^f} + \alpha \frac{mL^2}{(\overline{C}_L^f)^2} + \hat{C}_L \delta) \\
\leq& \frac{R^2}{m\alpha T} + O(\frac{R^{4/3} m^{-1/6} L^{5/2} \sqrt{\log m}}{\overline{C}_L^f} + \alpha \frac{mL^2}{(\overline{C}_L^f)^2} + \hat{C}_L \delta) \\
\leq& \epsilon
\end{aligned}
$$

Where the last inequality is due to parameter selection $\alpha = O(\frac{\epsilon (\overline{C}_L^f)^2}{mL^2})$, $T = \Theta(\frac{R}{m\alpha\epsilon})$, $m = \Omega(\frac{L^{16} R^9}{(\overline{C}_L^f)^7 \epsilon^7})$ and $\delta = O(\frac{\epsilon}{\hat{C}_L})$.

Given $\epsilon > 0$, suppose $R = \Omega(1)$ and $m = max(\Theta(\frac{L^{16} R^9}{(\overline{C}_L^f)^7 \epsilon^7}), \Theta(d^2))$. Let the loss function satisfy Assumption2. If we run projected gradient descent based on the convex constraint set $B(R)$ with step size $\alpha = O(\frac{\epsilon (\overline{C}_L^f)^2}{mL^2})$ for $T = \Theta(\frac{R}{m\alpha\epsilon})$ steps, with high probability we have

$$
\min_{0 \leq t \leq T} (Loss(\boldsymbol{W}^{(t)}, X') - Loss(\boldsymbol{W}^{(*)}, X)) \leq \epsilon
$$

where $\boldsymbol{W}^{(*)} = \arg\min_{\boldsymbol{W} \in B(R)} Loss(\boldsymbol{W}, X)$.

Table 8: Impacts of model depth (the number of layers). $\hat{C}_L$ is the factor deciding acceptable compression ratio (smaller is better).

| | Number of layers (L) | | | | |
|---|---|---|---|---|---|
| Factor | 2 | 3 | 5 | 10 | 20 |
| $\overline{C}_L^f$ | 0.1216 | 0.1095 | 0.0983 | 0.0804 | 0.0691 |
| $\overline{C}_L^e$ | 0.0152 | 0.0086 | 0.0047 | 0.0026 | 0.0018 |
| $\hat{C}_L$ | 0.1248 | 0.0788 | 0.0482 | 0.0325 | 0.0258 |

The selection of $m$, $\alpha$, and $\delta$ within the above analysis relies on factors decided by graph properties. For simplicity we can directly use the bounds of these factors so that $m = max(\Omega(\frac{L^{16}R^9n^7}{\epsilon^7}), \Omega(d^2))$, $\alpha = O(\frac{\epsilon}{mL^2n^2})$, and $\delta = O(\epsilon)$. The detailed analysis of these factors are in Section A.5.

### A.5 Impacts of Graph Structure and Model Depth on Compression Ratios

To train a GNN model over a large graph data set, the key to using feature quantization is to choose a proper compression ratio to strike a balance between the saved memory and PCIe bandwidth consumption and the accuracy. With the previous analysis of loss bound, combined with our experiments, we identify that the major contributor to the loss bound (see Theorem 3) is $\delta\hat{C}_L$. In particular, given an expected loss bound $\epsilon$, the factor $\hat{C}_L$ is inversely proportional to $\delta$, where $\delta$ is roughly $\Theta(2^{-32/CR})$. Therefore, we would expect the compression ratio to be negatively correlated to the $\hat{C}_L$. *Since $\hat{C}_L$ is relevant to both model depth, i.e., number of layers $L$, and the structure of the graph data set, we further study the impacts of the two factors on the selection of compression ratios.*

**Model depth.** We begin our analysis with understanding the impact of number of GNN layers. We test the values of $\overline{C}_L^f$ and $\overline{C}_L^e$ with the different numbers of layers on Reddit dataset. As expected, the values of $\overline{C}_L^f$ , $\overline{C}_L^e$, and $\hat{C}_L$ decrease when we increase the number of layers, as shown in Table8. The decrease in $\hat{C}_L$ is mainly because $\overline{C}_L^f$ decreases much slower than $\overline{C}_L^e$.

**Graph structure.** Then, to examine the impact of graph structure, we artificially create graph data sets with different structures based on the Reddit data set. Basically, we keep the Reddit nodes but delete some of the edges with three different selection methods to simulate graphs with varied sparsity, resulting in three types of data sets, namely, RANDOM, CENTRALIZED, and UNIFORM. In more detail, RANDOM deletes randomly selected edges, and thus keeps the power-law distribution of node degrees. CENTRALIZED deletes edges between low-degree nodes with high priority, leading the edges in the revised graph to be more centralized on high-degree nodes than that of the original graph. In contrast, UNIFORM prioritizes to delete edges between high-degree nodes, and make the resulting graph to follow an almost uniform degree distribution.

Table 9 shows the values of $\hat{C}_L$ with different graph structures under varied sparsity. Here, sparsity relates to the number of edges, i.e., more edges, denser graph, and vice versa. We also list the values of $\overline{C}_L^f$ and $\overline{C}_L^e$, as $\hat{C}_L = \overline{C}_L^e/\overline{C}_L^f$. Furthermore, $CR$ denotes the maximum compression ratio with less than 0.1% accuracy degradation. Note that, here, we use BiFeat-SQ for the analysis, where the maximum CR is 32.

We draw the following conclusions from Table 9. First, across the three data sets, denser graphs (higher percentage of remaining edges, in comparison to the original Reddit data set) always have smaller $\hat{C}_L$. Therefore, their compression ratios can be higher. With the same sparsity (the same percentage of remaining edges), the graphs created by the CENTRALIZED method have the following properties: some nodes are isolated, and the remaining nodes are connected by several super nodes. The direct consequence is to have a higher $\hat{C}_L$ and low acceptable compression ratio. Contrary, UNIFORM has a lower $\hat{C}_L$ and higher compression ratio. The reasons are as follows. The existence of super nodes makes the quantization errors spread to a large amount of nodes, which however can hardly be cancelled out during the aggregation, because neighbors of each node mainly have this component. But, the UNIFORM method addresses this limitation by eliminating super nodes and keeping each node's neighborhoods less overlapped.

Table 9: Impact of graph structures. CR means maximum acceptable compression ratio.

| Method to extract graph | | Percentage of remaining edges. 10% | 30% | 50% | 70% | 90% | 100% |
|---|---|---|---|---|---|---|---|
| RANDOM | $\overline{C}_L^f$ | 0.1329 | 0.1141 | 0.1147 | 0.1116 | 0.1050 | 0.1098 |
| | $\overline{C}_L^e$ | 0.0356 | 0.0171 | 0.0127 | 0.0105 | 0.0092 | 0.0088 |
| | $\hat{C}_L$ | 0.2677 | 0.1500 | 0.1109 | 0.0940 | 0.0875 | 0.0799 |
| | CR | 16 | 16 | 32 | 32 | 32 | 32 |
| CENTRALIZED | $\overline{C}_L^f$ | 0.4013 | 0.3789 | 0.3427 | 0.2836 | 0.1854 | |
| | $\overline{C}_L^e$ | 0.3873 | 0.3423 | 0.2924 | 0.2166 | 0.0913 | |
| | $\hat{C}_L$ | 0.9650 | 0.9034 | 0.8548 | 0.7638 | 0.4923 | |
| | CR | 4 | 4 | 8 | 16 | 16 | |
| UNIFORM | $\overline{C}_L^f$ | 0.1109 | 0.1111 | 0.1113 | 0.1022 | 0.1134 | |
| | $\overline{C}_L^e$ | 0.0169 | 0.0104 | 0.0089 | 0.0086 | 0.0087 | |
| | $\hat{C}_L$ | 0.1523 | 0.0938 | 0.0802 | 0.0845 | 0.0770 | |
| | CR | 32 | 32 | 32 | 32 | 32 | |

In summary, the above results indicate that BiFeat training is especially useful to handle deeper GNNs and graphs with degree distribution that is not very centralized.

# B Detailed Setups of Experiments

In this section, we show the detailed setups corresponding to experiments presented in Section 5.

## B.1 Accuracy Validation

**Node Property Prediction.** For GraphSAGE, GAT, and ClusterGCN, we use the example code from DGL[1]. We changed GAT implementation to make it support neighbor sampling and able to train on giant graphs.

ClusterGCN's default implementation uses the subgraph of train set nodes for training, which has poor performance in OGBN-Papers100M. We change this implementation by using the subgraph including train set nodes' 1-hop neighbors.

For MLP model, we use a three-layer MLP with ReLU activation and dropout, where its hidden layer dimension is 256. The SQ and VQ setups are

The detailed hyperparameters are listed in Table 10. Not listed hyperparameters use the default value.

The SQ parameter means the BiFeat-SQ setup used in the test. Here all tests are done with this parameter as 1, meaning we only use the sign bit to indicate the original float32 number. The VQ parameter includes two numbers, $width$ and $length$, are shown with the format $width$ - $length$. These parameters mean the number of dimensions of each codebook entry and the number of entries in each codebook, they will be discussed in detail in AppendixC.

**Link Property Prediction.** We test GCN and GraphSAGE with the OGB example code. Two models both use the default setting. The detailed setups are shown in Table11 and Table12, with the same manner as node property prediction setups.

**Graph Property Prediction.** We used the DGL example code of GIN and added GCN implementation. In our tests, GCN uses the same setup as GIN. The detailed setups are shown in Table12. Due to the original features being one-hot codes, we didn't test BiFeat-SQ, and we used a much more aggressive BiFeat-VQ setup.

## B.2 Accleration and Giant Graph

The tests of training acceleration and giant graph support use the same hyperparameter setup as the accuracy validation. In these tests, unless stated otherwise, we use a single card for training, and 5-7 CPU workers do sampling, making sure sampling is not the bottleneck.

Table 10: Experimental setups for the node property prediction tasks

| Model | Hyperparameters | Datasets Reddit | OGBN-Papers100M | MAG240M |
|---|---|---|---|---|
| GraphSAGE | #layer | 2 | 3 | 3 |
| | #hidden | 64 | 256 | 256 |
| | fan out | 10,25 | 5,10,15 | 5,10,15 |
| | SQ | 1 | 1 | 1 |
| | VQ | 100-16384 | 16-2048 | 16-2048 |
| GAT | #layer | 2 | 3 | 3 |
| | #hidden | 64 | 256 | 256 |
| | fan out | 10,25 | 5,10,15 | 5,10,15 |
| | drop out | 0.2 | 0.25 | 0.25 |
| | lr | 0.003 | 0.005 | 0.001 |
| | SQ | 1 | 1 | 1 |
| | VQ | 51-1024 | 16-16384 | 16-2048 |
| ClusterGCN | #hidden | 128 | 256 | - |
| | psize | 1000 | 1000 | - |
| | batch size | 100 | 20 | - |
| | dropout | 0.25 | 0.1 | - |
| | lr | 0.05 | 0.001 | - |
| | SQ | 1 | 1 | - |
| | VQ | 37-256 | 16-2048 | - |
| MLP | #layer | 3 | 3 | 3 |
| | #hidden | 256 | 256 | 256 |
| | SQ | 1 | 1 | 1 |
| | VQ | 16-1024 | 16-8192 | 12-2048 |

Table 11: Experimental setups for the link property prediction tasks

| Model | Hyperparameters | Datasets OGBL-COLLAB | OGBL-PPA |
|---|---|---|---|
| GCN | #layer | 3 | 3 |
| | #hidden | 256 | 256 |
| | lr | 0.001 | 0.01 |
| | SQ | 1 | 1 |
| | VQ | 16-2048 | 16-2048 |
| GraphSAGE | #layer | 3 | 3 |
| | #hidden | 256 | 256 |
| | lr | 0.001 | 0.01 |
| | SQ | 1 | 1 |
| | VQ | 16-2048 | 16-2048 |

We use the code of PaGraph[31] to test the performance of caching. We made minor modifications to make it work efficiently in the newer DGL version and kept its static caching strategy. We reserve about 1GB of GPU memory and use all other free memory for cache. As a result, for OGBN-Papers100M, about 8% original features or all quantized features can be cached; for MAG240M, about 0.5% of original features or 12% of the quantized features can be cached.

For the MAG240M dataset, we use the example code from OGB to do preprocessing, generate authors' features by averaging their papers' features, and generate institutions' features with authors' features. At last, we convert the heterogeneous graph into an undirected homogeneous graph.

During the training of GraphSAGE and GAT on the MAG240M dataset with original features, the peak memory usage is about 420GB. Using multiple cards for training in this situation almost used up CPU resources and significantly increased sampling time cost. Increasing the number of CPU sampling workers won't help. This problem didn't happen when using BiFeat, due to peak memory usage being about 70GB and only about half of the CPU resources being used.

Table 12: Experimental setups for the graph property prediction tasks

| Model | Hyperparameters | Datasets PTC | MUTAG | PROTEINS | COLLAB |
|---|---|---|---|---|---|
| GCN | #GNN layer | 5 | 5 | 5 | 5 |
| | #MLP layer | 2 | 2 | 2 | 2 |
| | #hidden | 64 | 64 | 64 | 64 |
| | degree as label | false | false | false | true |
| | graph pooling type | sum | sum | sum | mean |
| | VQ | 19-16 | 7-4 | 17-16 | 367-256 |
| GIN | #GNN layer | 5 | 5 | 5 | 5 |
| | #MLP layer | 2 | 2 | 2 | 2 |
| | #hidden | 64 | 64 | 64 | 64 |
| | degree as label | false | false | false | true |
| | graph pooling type | sum | sum | sum | mean |
| | VQ | 19-16 | 7-4 | 17-16 | 367-256 |

# C Open Source Code and Installation Instructions

We publish our BiFeat code anonymously on GitHub at https://github.com/BiFeat/BiFeat. In addition, we provide a guideline for the hyperparameter tuning of BiFeat.

**BiFeat-SQ.** There is only one parameter needed to configure, that is, the number of bits used to indicate a number. Setting this to 1 bit is practical for most cases, where only positive or not matters. For other cases, 2-bit is usually enough. Though there are other setups like the percentage of long-tailed values to be clipped, they are not very important in such a low bit width.

BiFeat-SQ is also efficient as it needs no more than several minutes to quantize even the largest MAG240M dataset.

**BiFeat-VQ.** Recall that the theoretical compression ratio of BiFeat-VQ is $\frac{width*32}{\log_2 length}$, where $length$ is the number of entries in each codebook and $width$ is the dimension of each entry. There are $\lceil \frac{\#feature\ dimension}{width} \rceil$ codebooks in total. Here we do not count the size of codebooks for two reasons. First, its size is small compared with features. Second, it is always kept in GPU. Thus we do not need to move it between CPU and GPU memory.

We can see that $length$ has less impact on the compression ratio. In our experiments, increasing $length$ yields less accuracy degradation with almost the same compression ratio. However, a large $length$ would significantly increase the time cost of vector quantization. For MAG240M, it may take up to a whole day to perform compression. This is because BiFeat-VQ needs to calculate the pair-wise distance to choose a proper entry in the codebook for each node, and thus the time cost is proportional to the $length$. We observe the acceptable $length$ is at most 16384. Thus each vector needs 2 bytes to store the index of the codebook entry due to bit alignment. Without a highly complex method to pack bits, we advise using a $length$ of 256 for convenience, paired with a width capable of reaching the optimal accuracy while as big as possible. This would also save the pre-processing time, sacrificing maximum compression ratio.

# D Discussions on Time Cost of Feature Quantization

We did not fully discuss the pre-processing time for quantizing feature data in our submission. This is because it depends on the compression method and the choice of compression parameters. For BiFeat-SQ, it is very efficient. Even when processing the MAG240M dataset (up to 375GB), it takes no more than 15 minutes using the highest compression rate. However, for BiFeat-VQ, it takes hours to process the MAG240M dataset because of the calculation of the global information. To accelerate BiFeat-VQ pre-processing, we uniformly sample a portion of the data instead of global data for statistics. The uniform random sampling strategy we use may not be optimal as the features are accessed unevenly in GNN training. We plan to explore other strategies in our future work. In addition, it is more efficient to use the GPU to accelerate BiFeat-VQ pre-processing. We also leave this as our future work.